Supplemental Material for Deformation versus sphericity in the ground states of the lightest gold isotopes

J. G. Cubiss,[1,][*] A. N. Andreyev,[1, 2] A. E. Barzakh,[3] P. Van Duppen,[4] S. Hilaire,[5] S. Péru,[5] S. Goriely,[6] M. Al Monthery,[1]
N. A. Althubiti,[7, 8] B. Andel,[9] S. Antalic,[9] D. Atanasov,[10, 11] K. Blaum,[10] T. E. Cocolios,[7, 4] T. Day Goodacre,[7, 11, †]
A. de Roubin,[10, ‡] G. J. Farooq-Smith,[7, 4] D. V. Fedorov,[3] V. N. Fedosseev,[11] D. A. Fink,[11, 10] L. P. Gaffney,[4, 11, §] L. Ghys,[4, ¶]
R. D. Harding,[1, 11] M. Huyse,[4] N. Imai,[12] D. T. Joss,[13] S. Kreim,[11, 10] D. Lunney,[14, **] K. M. Lynch,[7, 11] V. Manea,[10, **]
B. A. Marsh,[11] Y. Martinez Palenzuela,[4, 11] P. L. Molkanov,[3] D. Neidherr,[15] G. G. O'Neill,[13] R. D. Page,[13] S. D. Prosnyak,[3]
M. Rosenbusch,[16] R. E. Rossel,[11, 17] S. Rothe,[11, 17] L. Schweikhard,[16] M. D. Seliverstov,[3] S. Sels,[4] L. V. Skripnikov,[3]
A. Stott,[1] C. Van Beveren,[4] E. Verstraelen,[4] A. Welker,[11, 18] F. Wienholtz,[11, 16, ††] R. N. Wolf,[10, 16, ‡‡] and K. Zuber[18]

[1]*School of Physics, Engineering and Technology, University of York, York, YO10 5DD, United Kingdom*
[2]*Advanced Science Research Center (ASRC), Japan Atomic Energy Agency, Tokai-mura, Japan*
[3]*Affiliated with an institute covered by a cooperation agreement with CERN*
[4]*KU Leuven, Instituut voor Kern- en Stralingsfysica, 3001 Leuven, Belgium*
[5]*Université Paris-Saclay, CEA, LMCE, 91680, Bruyères-le-Châtel, France*
[6]*Institut d'Astronomie et d'Astrophysique, CP-226, Université Libre de Bruxelles, 1050 Brussels, Belgium*
[7]*The University of Manchester, School of Physics and Astronomy, Oxford Road, M13 9PL Manchester, United Kingdom*
[8]*Physics Department, College of Science, Al-jouf University, Sakakah, Kingdom of Saudi Arabia*
[9]*Department of Nuclear Physics and Biophysics, Comenius University in Bratislava, 84248 Bratislava, Slovakia*
[10]*Max-Planck-Institut für Kernphysik, Saupfercheckweg 1, 69117 Heidelberg, Germany*
[11]*CERN, 1211, Geneva 23, Switzerland*
[12]*Center for Nuclear Study (CNS), Graduate School of Science The University of Tokyo, Japan*
[13]*Department of Physics, University of Liverpool, Liverpool, L69 7ZE, United Kingdom*
[14]*CSNSM-CNRS, Université de Paris Sud, 91400 Orsay, France*
[15]*GSI Helmholtzzentrum für Schwerionenforschung GmbH, Darmstadt 64291, Germany*
[16]*Institut für Physik, Universität Greifswald, 17487 Greifswald, Germany*
[17]*Institut für Physik, Johannes Gutenberg-Universität Mainz, Mainz, D-55128, Germany*
[18]*Institut für Kern- und Teilchenphysik, Technische Universität Dresden, Dresden 01069, Germany*

Fitting hyperfine structure spectra and calculation of electronic factors

Figure 1 shows the three-step ionization scheme used to produce gold ions during the experiment. The hyperfine structure (hfs) and isotope shift (IS) measurements were performed on the 267.6 nm, $6s\,^2S_{1/2} \rightarrow 6p\,^2P^o_{1/2}$ atomic transition. The components of the hfs were fitted with Voigt profiles using a χ-squared minimisation, where their positions are given by the expression [1]:

$$\nu^{F,F'} = \nu + a_{6p}\frac{C'}{2} - a_{6s}\frac{C}{2}, \quad (1)$$

where ν is the transition's centroid frequency, $C = F(F + 1) - I(I + 1) - J(J + 1)$, I, J and F are the total angular momenta of the nuclear, electronic, and atomic levels, respectively, $a_{n\ell}$ is the magnetic hyperfine constant for the atomic level with quantum numbers n and ℓ, and the prime symbol denotes the upper level of the atomic transition. The positions of the hfs components were determined using four parameters: the nuclear spin, I; the isotope shift (IS) relative to stable ^{197}Au ($\delta\nu_{A,197} = \nu_A - \nu_{197}$); and the magnetic hfs constants, a_{6s} and a_{6p}, for the lower and upper levels involved in the transition scanned using the narrowband laser[1]. Transition intensities

were fitted using calculated Racah coefficients, accounting for differences in the saturation of hfs components in the first and second step of the laser ionization scheme (see Ref. [2] for details).

From the fits, values for the IS between specific states and the ground state of ^{197}Au were extracted. These were used to deduce $\delta\langle r^2\rangle_{A,197}$ values using the relation:

$$\delta\nu_{A,197} = (k_{\mathrm{NMS}} + k_{\mathrm{SMS}})\left(\frac{1}{M_A} - \frac{1}{M_{197}}\right) + \mathcal{F}\delta\langle r^2\rangle_{A,197}, \quad (2)$$

where $\mathcal{F}$ is an electronic factor, k_{NMS} is the normal mass shift (NMS) constant, and k_{SMS} is the specific mass shift (SMS) constant, and M_A is the atomic mass of the isotope with mass number A.

Previous IS studies of gold nuclei used a value of $\mathcal{F} = -43.07$ GHz/fm^2 for the 267.6-nm transition [4–10]. This was calculated within the framework of the multi-configuration Dirac-Fock theory. However, no estimations of the theoretical uncertainty were given. Empirically estimated theoretical uncertainties proposed by Otten [1] for $\mathcal{F}$ (of $\approx 10\%$, or more in

---

[1] As both atomic levels in the $6s\,^2S_{1/2} \rightarrow 6p\,^2P^o_{1/2}$ transition have $J = 1/2$, the quadrupole hfs constants $\equiv 0$. Hence, it is not possible to extract spec-

troscopic quadrupole moments from our data. Nuclear spins could not be unambiguously determined from our hfs spectra, due to our limited resolution. Therefore, they were fixed according to values taking from literature, or from our complementary decay studies.
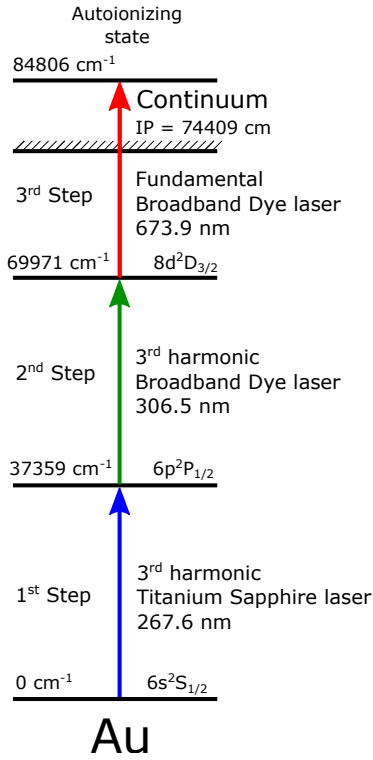
FIG. 1. The three-step ionization scheme used during the experiment to produce gold ions (adapted from Ref. [3]).

some cases), are far larger than the precision achieved experimentally. Indeed, our recent works have shown that in some cases, the values from old calculations require corrections of the order of $\sim 20\%$ compared to advanced methods [11]. Furthermore, in previous works the k_{SMS} constant for the 267.6-nm transition was not calculated at all [5, 6]. Instead, a global empirical estimation for all $ns \rightarrow np$ transitions was used ($k_{SMS} = (0.3 \pm 0.9)k_{NMS}$ [12]). Therefore, considering the advances in atomic calculations since the previous works, and the need for proper evaluation of the associated uncertainties, new calculations to determine the values of $\mathcal{F}$, k_{NMS} and k_{SMS} were performed.

The constants k_{NMS} and k_{SMS} were calculated using the following relativistic Hamiltonians [13–16]:

$$H_{\text{NMS}} = \frac{1}{2A} \sum_i (\vec{p}_i^2 - \frac{\alpha Z}{r_i} \left[\vec{\alpha}_i + \frac{(\vec{\alpha}_i \cdot \vec{r}_i)\vec{r}_i}{r_i^2} \right] \cdot \vec{p}_i), \quad (3)$$

$$H_{\text{SMS}} = \frac{1}{2A} \sum_{i \neq k} (\vec{p}_i \cdot \vec{p}_k - \frac{\alpha Z}{r_i} \left[\vec{\alpha}_i + \frac{(\vec{\alpha}_i \cdot \vec{r}_i)\vec{r}_i}{r_i^2} \right] \cdot \vec{p}_k), \quad (4)$$

where Z is the proton number, $\vec{\alpha}_i$ are Dirac matrices corresponding to electron i and $\vec{r}_i$ is the coordinate of ith electron. Electronic correlation effects have been considered within the relativistic coupled cluster theory with inclusion up to quadruple cluster amplitudes [17–19]. In the electronic structure calculations, we have used the uncontracted Gaussian type

Dyall's [20, 21] basis sets augmented by additional basis functions. Basis sets LHbas and Lbas correspond to the extended uncontracted AE4Z Dyall's basis set, while Mbas and Sbas basis sets correspond to the extended uncontracted AE3Z and AE2Z Dyall's basis sets, respectively. Compositions of employed basis sets are given in descending order of their quality in Table I.

For electronic structure calculations the locally modified DIRAC15 [22, 23], MRCC [18, 19, 24], Exp-T [25, 26] and HFD [27–29] codes have been used.

TABLE I. The total number of basis functions in different basis sets.

Basis set	Functions
LHbas	$40s$, $36p$, $19d$, $14f$, $10g$, $7h$, $4i$
Lbas	$40s$, $36p$, $19d$, $14f$, $10g$, $5h$, $1i$
Mbas	$36s$, $30p$, $15d$, $11f$, $5g$, $1h$
Sbas	$30s$, $25p$, $12d$, $9f$, $1g$

Calculated contributions to the field shift and mass shift constants are given in Table II. The main correlation calculations have been performed using the coupled cluster method with single, double, and perturbative triple amplitudes, CCSD(T) [30, 31], the Dirac-Coulomb Hamiltonian and the Gaussian nuclear charge distribution model. The LHbas basis set has been employed for the case of $\mathcal{F}$ and k_{NMS} constants. Calculation of the mass shift constant k_{SMS} is technically more complicated due to the two-electron nature of the corresponding operator. Therefore, in this case, the Mbas basis set has been used. All electrons were included in the correlation treatment. The virtual orbitals were truncated at the energy of 10000 E_h. Calculations of the contributions of correlation effects beyond the CCSD(T) model have been performed within the coupled cluster with single, double, triple, and perturbative quadruple amplitudes, CCSDT(Q), method [17–19] within the Mbas basis set. In these calculations, sixty $1s - 4f$ electrons were excluded from the correlation treatment and virtual energy cutoff has been set to 20 E_h. For k_{SMS} we have calculated basis set correction at the CCSD level as the difference between the k_{SMS} values obtained in all-electron calculations using Lbas and Mbas basis sets. The contribution of the Gaunt interelectron interaction has been calculated at the self-consistent field level. Note, that the non-relativistic NMS, $k_{\text{NMS}} = \nu/1822.9 = 615$ GHz u (ν being the transition frequency), is very close to our relativistic value (see Table II), however, it is not possible to estimate the uncertainty in the non-relativistic case.

The uncertainties on the calculated constants consist of several terms. The contributions of the effect of increasing the basis set from MBas to LHBas (for the case of $\mathcal{F}$ and k_{NMS}) and to LBas (for the case of k_{SMS}) have been used as an estimate of the uncertainty due to the basis set quality. The Gaunt interaction contribution given in Table II is included totally in the uncertainty. The uncertainty due to correlation effects takes into account: (i) higher-order correlation effects uncertainty for sixty core electrons, estimated as the difference between contributions of non-iterative triple amplitudes for all

TABLE II. Calculated values of the normal, k_{NMS}, specific, k_{SMS}, total, k_{Total} mass shift constants (in GHz·a.m.u.), and the field shift constant, $\mathcal{F}$, (in GHz/fm^2) using different levels of electronic theory.

	k_{NMS}	k_{SMS}	k_{Total}	$\mathcal{F}$
79e-CCSD(T)	723	221	944	-41.9
19e-CCSDT - 19e-CCSD(T)	-124	-37	-161	+1.0
19e-CCSDT(Q) - 19e-CCSDT	-4	-31	-35	+0.5
Basis set correction	–	-28	-28	–
Gaunt	+5	-22	-17	+0.3
Total	600(40)	103(93)	703(101)	-40.1(11)

electrons and 19 valence electrons; (ii) higher-order correlation effects uncertainty for 19 valence electrons estimated as the "CCSDT(Q)-CCSDT" correction; (iii) the uncertainty of the "CCSDT(Q)-CCSD(T)" contribution, estimated as the difference between the values of these contributions calculated in the Mbas and the Sbas basis sets. This term corresponds to the "interference" between high-order correlation effects and the basis set size increase effect. For the $\mathcal{F}$ constant (for which we obtained results with smaller uncertainty) we have also estimated the uncertainty due to the nuclear charge distribution model (Gauss vs. Fermi) at the self-consistent field level. Finally, following Ref. [11] we include effects of QED of $\approx 1\%$ in the uncertainty of $\mathcal{F}$. The total uncertainty was determined by summing the different contributions in quadrature. For $\mathcal{F}$, the different contributions to the uncertainty are 1.2% from the electron correlation treatment level, 1.5% from the finite basis set limitations, 0.7% from the Gaunt contribution uncertainty, and 1% from the nuclear charge distribution. For the mass shift constants, uncertainties of: 1.7% for k_{NMS}, 27.7% for k_{SMS} stem from the finite basis set; 6.4% for k_{NMS}, 83.0% for k_{SMS} from the correlation effects treatment; and 0.9% for k_{NMS}, 21.3% for k_{SMS} from the Gaunt contribution.

Comparison of experimental and calculated magnetic dipole moments for gold isotopes
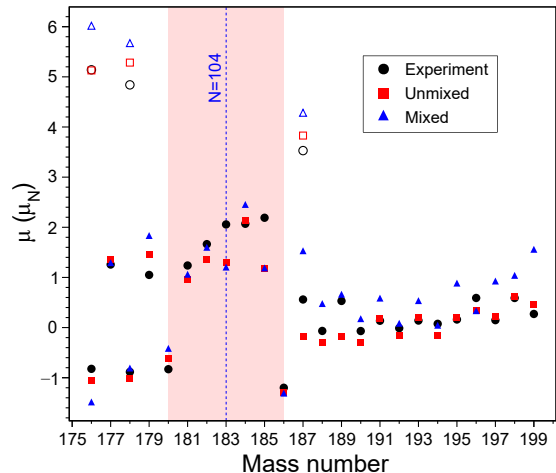

FIG. 2. Comparison between experimental magnetic dipole moments (●) of gold isotopes with those from HFB calculation without (■) and with (▲) configuration mixing included. The filled symbols indicate ground states, whilst the hollow symbols represent the isomers in ^{178,187}Au and the high-spin state in ^{176}Au. The shaded pink area is to guide the eye, and indicates the region of well-deformed ground states.

Comparison of experimental and calculated changes in mean-squared charge radii in the lead region
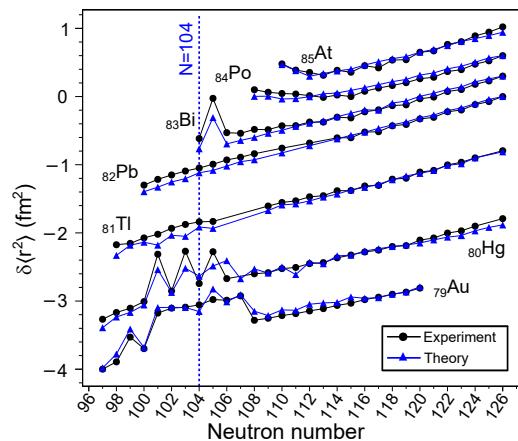

FIG. 3. Comparison between experimental (●) and theoretical (▲) results for ground state $\delta\langle r^2 \rangle$ values along isotopic chains. Candidates states were selected from the calculations based on having the best agreement with $\delta\langle r^2 \rangle$, correct I^π when compared to experiment, a μ value within 50% agreement of the experimental value, and an excitation energies within 2 MeV of the calculated ground state. The isotopic chains are arbitrarily offset from each other for clarity, and are labelled with their chemical symbol and proton number.

* james.cubiss@york.ac.uk
† Present address: TRIUMF, Vancouver BC V6T 2A3, Canada

‡ Present address: Centre d'Etudes Nucléaires de Bordeaux-Gradignan, 19 Chemin du Solarium, CS 10120, F-33175 Gradignan,France

§ Present address: Department of Physics, University of Liverpool, Liverpool, L69 7ZE, United Kingdom

¶ Present address: Belgian Nuclear Research Center SCK CEN, Boeretang 200, B-2400 Mol, Belgium

** Present address: Université Paris-Saclay, CNRS/IN2P3, IJCLab, 91405 Orsay, France

†† Present address: Institut für Kernphysik, Technische Universität Darmstadt, 64289 Darmstadt, Germany

‡‡ Present address: ARC Centre of Excellence for Engineered Quantum Systems, The University of Sydney, NSW 2006, Australia

[1] E. W. Otten, in *Treatise on Heavy Ion Science*, edited by D. A. Bromley (Springer US, Boston, MA, 1989) 1st ed., Chap. 7, pp. 517–638.

[2] M. D. Seliverstov, T. E. Cocolios, W. Dexters, A. N. Andreyev, S. Antalic, A. E. Barzakh, B. Bastin, J. Büscher, I. G. Darby, D. V. Fedorov, V. N. Fedosseev, K. T. Flanagan, S. Franchoo, G. Huber, M. Huyse, M. Keupers, U. Köster, Y. Kudryavtsev, B. A. Marsh, P. L. Molkanov, R. D. Page, A. M. Sjödin, I. Stefan, P. Van Duppen, M. Venhart, and S. G. Zemlyanoy, Physical Review C **89**, 034323 (2014).

[3] B. A. Marsh, V. N. Fedosseev, and P. Kosuri, Hyperfine Interactions **171**, 109 (2006).

[4] C. Ekström, L. Robertsson, S. Ingelman, G. Wannberg, and I. Ragnarsson, Nuclear Physics A **348**, 25 (1980).

[5] K. Wallmeroth, G. Bollen, A. Dohn, P. Egelhof, J. Grüner, F. Lindenlauf, U. Krönert, J. Campos, A. Rodriguez Yunta, M. J. G. Borge, A. Venugopalan, J. L. Wood, R. B. Moore, and H. J. Kluge, Physical Review Letters **58**, 1516 (1987).

[6] K. Wallmeroth, G. Bollen, A. Dohn, P. Egelhof, U. Krönert, M. J. G. Borge, J. Campos, A. R. Yunta, K. Heyde, C. De Coster, J. L. Wood, and H. J. Kluge, Nuclear Physics, Section A **493**, 224 (1989).

[7] U. Krönert, S. Becker, G. Bollen, M. Gerber, T. Hilberath, H. J. Kluge, and G. Passler, Zeitschrift für Physik A Atomic Nuclei **331**, 521 (1988).

[8] G. Savard, J. Crawford, J. Lee, G. Thekkadath, H. Duong, J. Pinard, F. Le Blanc, P. Kilcher, J. Obert, J. Oms, J. Putaux, B. Roussiere, and J. Sauvage, Nuclear Physics A **512**, 241 (1990).

[9] G. Passler, J. Rikovska, E. Arnold, H.-J. Kluge, L. Monz, R. Neugart, H. Ravn, and K. Wendt, Nuclear Physics A **580**, 173 (1994).

[10] F. Le Blanc, J. Obert, J. Oms, J. C. Putaux, B. Roussière, J. Sauvage, J. Pinard, L. Cabaret, H. T. Duong, G. Huber, M. Krieg, V. Sebastian, J. Crawford, J. K. P. Lee, J. Genevey, and F. Ibrahim, Physical Review Letters **79**, 2213 (1997).

[11] G. Penyazkov, S. D. Prosnyak, A. E. Barzakh, and L. V. Skripnikov, The Journal of Chemical Physics **158**, 114110 (2023).

[12] K. Heilig and A. Steudel, Atomic data and nuclear data tables **14**, 1 (1974).

[13] V. M. Shabaev, Theor. Math. Phys. **63**, 588 (1985).

[14] C. W. P. Palmer, Journal of Physics B: Atomic and Molecular Physics **20**, 5987 (1987).

[15] V. M. Shabaev, Sov. J. Nucl. Phys. **47**, 69 (1988).

[16] V. Shabaev and A. Artemyev, Journal of Physics B: Atomic, Molecular and Optical Physics **27**, 1307 (1994).

[17] M. Kállay and J. Gauss, J. Comp. Phys. **123**, 214105 (2005).

[18] M. Kállay and P. R. Surján, J. Comp. Phys. **115**, 2945 (2001).

[19] M. Kállay, P. G. Szalay, and P. R. Surján, J. Comp. Phys. **117**, 980 (2002).

[20] K. G. Dyall, Theor. Chem. Acc. **115**, 441 (2006).

[21] K. G. Dyall, Theor. Chem. Acc. **99**, 366 (1998).

[22] DIRAC, a relativistic ab initio electronic structure program, Release DIRAC15 (2015), written by R. Bast, T. Saue, L. Visscher, and H. J. Aa. Jensen, with contributions from V. Bakken, K. G. Dyall, S. Dubillard, U. Ekstroem, E. Eliav, T. Enevoldsen, E. Fasshauer, T. Fleig, O. Fossgaard, A. S. P. Gomes, T. Helgaker, J. Henriksson, M. Ilias, Ch. R. Jacob, S. Knecht, S. Komorovsky, O. Kullie, J. K. Laerdahl, C. V. Larsen, Y. S. Lee, H. S. Nataraj, M. K. Nayak, P. Norman, G. Olejniczak, J. Olsen, Y. C. Park, J. K. Pedersen, M. Pernpointner, R. Di Remigio, K. Ruud, P. Salek, B. Schimmelpfennig, J. Sikkema, A. J. Thorvaldsen, J. Thyssen, J. van Stralen, S. Villaume, O. Visser, T. Winther, and S. Yamamoto (see http://www.diracprogram.org).

[23] R. Saue, T. Bast, A. S. P. Gomes, H. J. A. Jensen, L. Visscher, I. A. Aucar, R. Di Remigio, K. G. Dyall, E. Eliav, E. Fasshauer, T. Fleig, L. Halbert, E. D. Hedegard, B. Helmich-Paris, M. Ilias, C. R. Jacob, S. Knecht, J. K. Laerdahl, M. L. Vidal, M. K. Nayak, M. Olejniczak, J. M. H. Olsen, M. Pernpointner, B. Senjean, A. Shee, A. Sunaga, and J. N. P. van Stralen, J. Chem. Phys. **152**, 204104 (2020).

[24] "mrcc," M. Kállay, P. R. Nagy, D. Mester, Z. Rolik, G. Samu, J. Csontos, J. Csóka, P. B. Szabó, L. Gyevi-Nagy, B. Hégely, I. Ladjánszki, L. Szegedy, B. Ladóczki, K. Petrov, M. Farkas, P. D. Mezei, and á. Ganyecz: The mrcc program system: Accurate quantum chemistry from water to proteins, J. Chem. Phys. 152, 074107 (2020). mrcc, a quantum chemical program suite written by M. Kállay, P. R. Nagy, D. Mester, Z. Rolik, G. Samu, J. Csontos, J. Csóka, P. B. Szabó, L. Gyevi-Nagy, B. Hégely, I. Ladjánszki, L. Szegedy, B. Ladóczki, K. Petrov, M. Farkas, P. D. Mezei, and á. Ganyecz. See www.mrcc.hu.

[25] A. V. Oleynichenko, A. Zaitsevskii, and E. Eliav, in *Supercomputing*, Vol. 1331, edited by V. Voevodin and S. Sobolev (Springer International Publishing, Cham, 2020) pp. 375–386.

[26] A. Oleynichenko, A. Zaitsevskii, and E. Eliav, (2021), EXP-T, an extensible code for Fock space relativistic coupled cluster calculations (see http://www.qchem.pnpi.spb.ru/expt) (accessed on 4 February 2022).

[27] I. I. Tupitsyn, G. B. Deyneka, and V. F. Bratzev, "hfd," (1977–2002), hfd, a program for atomic finite-difference four-component Dirac-Hartree-Fock calculations on the base of the HFD code [29].

[28] I. I. Tupitsyn, "hfdb," (2003), hfdb, a program for atomic finite-difference four-component Dirac-Hartree-Fock-Breit calculations written on the base of the hfd code [29].

[29] V. F. Bratzev, G. B. Deyneka, and I. I. Tupitsyn, Bull. Acad. Sci. USSR, Phys. Ser. **41**, 173 (1977).

[30] L. Visscher, T. J. Lee, and K. G. Dyall, J. Comp. Phys. **105**, 8769 (1996).

[31] R. J. Bartlett and M. Musiał, Rev. Mod. Phys. **79**, 291 (2007).